Hindawi Publishing Corporation
ISRN Optics
Volume 2013, Article ID 986924, 9 pages
http://dx.doi.org/10.1155/2013/986924

Research Article

Circular Photonic Crystal Fibers: Numerical Analysis of Chromatic Dispersion and Losses

Partha Sona Maji and Partha Roy Chaudhuri

Department of Physics and Meteorology, Indian Institute of Technology, Kharagpur 721302, India

Correspondence should be addressed to Partha Sona Maji; parthamaji.1984@gmail.com

Received 8 August 2013; Accepted 10 September 2013

Academic Editors: G. Bellanca, M. D. Hoogerland, Y. S. Kivshar, and G. S. Maciel

Detailed numerical analysis for dispersion properties and losses has been carried out for a new type of Photonic crystal fiber where the air-holes are arranged in a circular pattern with a silica matrix called as Circular Photonic Crystal Fiber (C-PCF). The dependence of different PCF geometrical parameters namely different circular spacings, air-hole diameter and numbers of air-hole rings are carried out in detail towards practical applications. Our numerical analysis establishes that total dispersion is strongly affected by the interplay between material dispersion and waveguide dispersion. For smaller air-filing fraction, adding extra air-hole rings does not change dispersion much whereas for higher air-filling fraction, the dispersion nature changes significantly. With proper adjustment of the parameters ultra-flattened dispersion could be achieved; though the application can be limited by higher losses. However, the ultra-flat dispersion fibers can be used for practical high power applications like supercontinuum generation (SCG) by reducing the loss at the pumping wavelength by increasing the no of air-hole rings. Broadband smooth SCG can also be achieved with low loss oscillating near-zero dispersion fiber with higher no of air-hole rings. The detail study shows that for realistic dispersion engineering we need to be careful for both loss and dispersion.

1. Introduction

Photonic crystal fibers (PCFs) or microstructured optical fibers (MOFs) [1, 2] are special types of optical fiber where air holes are arranged in a periodic nature in the cladding. These types of fibers possess some novel guiding properties, related to the geometric characteristics of the air holes in their cross-section and have been successfully exploited in different applications [1, 2]. Most of the air holes in the PCFs cladding have been arranged either in a periodic triangular or periodic square orientation. The modal properties, in particular, and the dispersion properties of the above types of PCFs can be altered by varying the hole-to-hole spacing (Λ) and the air hole diameter (d) with air-filling fraction being d/Λ [3, 4]. Both types of PCFs with a silica background can be successfully implemented to compensate the positive dispersion parameter and dispersion slope of the existing inline fibers [3, 4]. These fibers can be engineered for designing ultraflattened near-zero dispersion [5–7] or can be engineered to have ultranegative dispersion values near the communication wavelength [8–10].

Recently, there have been new types of cross-sectional geometry where air holes are arranged in a circular pattern [11–16]. Photonic Crystal with air holes arranged in circular layer arrangements has been investigated for different applications [11–15] such as studying thermal properties for electrical driving [11], high transmission waveguides [12], high quality factor microcavity lasers with isotropic photonic band gap effect [13], localization of electromagnetic waves [14] and achieving ultraflat dispersion [15], and so forth. Argyros et al. [16] realized PCF with circular air holes arrangement with polymer background. Though the above works based on C-PCF demonstrate few researches that have been accomplished, still a detailed guiding and modal properties based on the geometrical parameters of C-PCF with silica background have not yet been explored for its potential applications in the communication wavelength window or infrared (IR) or far-IR applications.

In this work, we have made a detailed numerical analysis of the dispersion and loss property of the C-PCF for the first time. We have considered different circular spacings, air hole diameter, and different numbers of air hole rings (N_r). The detailed study will be useful for practical engineering applications where both loss and dispersion play an integral part.

2. Geometry of the Studied Structure and Modal Analysis

The schematic diagram of the C-PCF is shown in Figure 1 with the air hole diameter as d and the radius of the circles, as well as the spacing between the rings, is R. The C-PCF, where air holes are arranged in a circle of certain radius is constructed by repeating the circular unit around the core center. The circles have $6n$ (with $n = 1, 2, 3$, and so forth for first, second, and third rings of air holes) number of air holes in a particular air hole ring. The angular spacing between any two consecutive air holes in a circle can be given by $\theta = 360/6n$, where $n = 1, 2, 3$, and so forth for first, second, and third layers of the circles forming the cladding cross-section. The structure under investigation is having twofold symmetry (C_{2v} symmetry). We compare the propagation characteristics of circular-lattice PCF with triangular-lattice PCF for the structural parameters; the pitch "Λ" (hole-to-hole distance of regular triangular-lattice PCF) is found to have the direct equivalence with "R" (the radius of the circle and the distance between two consecutive circles). Thus, employing the above analogy under the same air hole diameter d, d/Λ (the air-filling fraction) for triangular PCF can be compared with d/R of C-PCF. Another important geometrical parameter is air-filling fraction f. The corresponding value for triangular-lattice PCF is $f_\Delta = (\pi d^2)/(2\sqrt{3}\Lambda^2) = 0.9069(d^2/\Lambda^2)$ [4], whereas for the C-PCF the value comes out to be $f_\circ \approx (6\pi d^2)/(8R^2) \approx 0.75(d^2/R^2)$. So C-PCF is having an air-filling factor which is 82% compared to that of triangular lattice PCF. With the lower index of the air-filled cladding and the higher index of the silica fiber core (the center air hole being missing), the propagation modes can exist due to the modified total internal reflection (TIR) mechanism in this type of PCF structure. The modal fields are calculated using CUDOS MOF utilities [17] that simulates PCFs using the multipole method [18, 19]. The validity and efficiency of the method has already been established [18, 19]. The numerical calculations, namely, dispersion parameter (D) and losses (L), are calculated with MATLAB. The guiding properties of the C-PCF have been studied in the following section by taking into consideration of the various combinations of radius of the circle and air hole diameter. We discuss the modal properties in the subsequent sections as follows.

3. Propagation Characteristics: Results and Analysis

PCFs, with the ability to change their different geometrical parameters, possess the unique and attractive applications like dispersion tailoring [3], endlessly single-mode operation [20], and higher nonlinearity [21] which are not achievable in standard silica fibers. Controllability of waveguide dispersion in PCFs is an important issue for applications of optical communications, dispersion compensation, nonlinear applications, and so forth. The dispersion property for PCFs with regular triangular lattice and square lattice can be controlled by varying the d and Λ [3, 4]. Similarly, for C-PCF, the dispersion can be controlled by varying the radius of the circle R and air hole diameter d and number of air hole rings (N_r). We have calculated the dispersion parameter (D) of the structures through

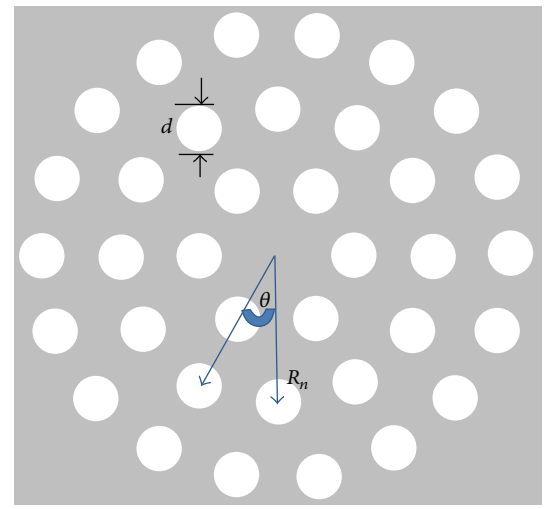

Figure 1: The schematic diagram of the studied fiber. Air holes are arranged equally spaced in a circular pattern of radius R in silica background.

$$D = -\frac{\lambda}{c}\frac{d^2\,\mathrm{Re}\left[n_{\mathrm{eff}}\right]}{d\lambda^2}. \tag{1}$$

Here $\mathrm{Re}[n_{\mathrm{eff}}]$ is the real part of the effective indices obtained from the simulation, and c is the velocity of light in vacuum.

The confinement loss for the structures has been calculated through

$$L = \frac{2\pi}{\lambda}\frac{20}{\ln(10)}10^6\,\mathrm{Im}\left(n_{\mathrm{eff}}\right)\frac{dB}{m}, \tag{2}$$

where $\mathrm{Im}(n_{\mathrm{eff}})$ is the imaginary part of the effective indices (obtained from the simulations) and λ in micrometer. The chromatic dispersion of the background silica material has been taken into account through Sellmeier's equation.

3.1. Dispersion Properties. We studied the dispersion and loss property of the C-PCF for a broad wavelength range from 0.8 μm to 2.8 μm. Figure 2 shows the dispersion property taking into consideration equal air hole diameter (we have taken it to be 0.80 μm), for different values of circular spacing (R) with $N_r = 3$. The figure shows that for smallest values of the radius of the circle ($R = 1.50\ \mu$m) the dispersion property is oscillating in the whole wavelength range and few numbers

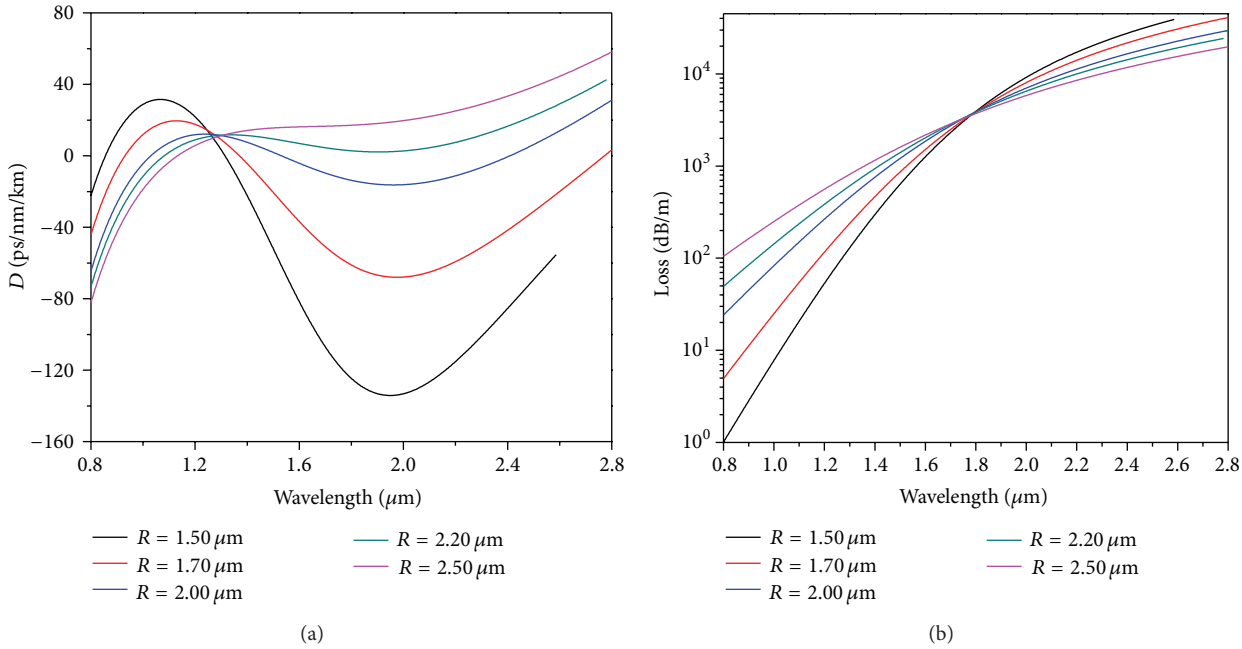

FIGURE 2: (a) Dispersion and (b) losses for different spacings of the circle (R) for three-ring C-PCF with air hole diameter $d = 0.8\,\mu$m.

of zero-dispersion wavelengths can be found. As we increase the value of R, the oscillating nature gradually disappears. Instead, a monotonically increasing nature of the dispersion could be found out. This typical nature of the dispersion can be explained on the basis of the interplay between the material dispersion and waveguide effect upon the dispersion. For smaller values of R, the waveguide nature dominates, which results in an oscillating nature of the dispersion. The figure clearly indicates that the smaller the values of the radius of the circle, the larger the magnitude of oscillation. For all cases of R, for smaller wavelength the dispersion values are always negative. This is because of the fact that, for smaller values of wavelength, the material dispersion is so negative that the waveguide dispersion just cannot compensate the material one. This characteristic justifies that for smaller wavelengths all the dispersion tends towards the material one.

3.1.1. Ultraflat Dispersion and Its Dependence Upon N_r. An interesting observation that follows by observing from Figure 2 is that, for $R = 2.40\,\mu$m, the dispersion value is almost flat (average D value of 13.5 ps/nm/km around 1.65 μm of wavelength) over a long wavelength range (from 1.38 μm to 1.91 μm, i.e., wavelength band of almost 530 nm) with the dispersion oscillation of 0.35 ps/nm/km. For $N_r = 4$,without changing the other design parameters, we could observe that the oscillation increases to 1.75 ps/nm/km (with wavelength band of 880 nm) with the average $D = 8.25$ ps/nm/km around 1.61 μm as shown in Figure 3(a). With the same parameter, the flatness reduces (i.e., the oscillation increases) with the dispersion oscillation of 3.3 ps/nm/km and 4.5 ps/nm/km for $N_r = 5$ and $N_r = 6$ as shown in Figures 4(a) and 5(a), respectively. However, we could achieve flat dispersion with $D = 9.75$ ps/nm/km (with dispersion fluctuation of 0.45 ps/nm/km around 1.63 μm) with $N_r = 6$ and $R = 2.6\,\mu$m. Another interesting observation can be found out from Figure 2(a) regarding the dispersion variation with $R = 2.10\,\mu$m. The dispersion oscillates around zero dispersion with $D = 0 \pm 11.2$ ps/nm/km for a wavelength bandwidth of 1460 nm. Similar nature can be observed with $N_r = 4$ ($D = 0 \pm 9.1$ ps/nm/km, wavelength bandwidth of 1380 nm with $R = 2.20\,\mu$m), $N_r = 5$ ($D = 0 \pm 8.3$ ps/nm/km, wavelength bandwidth of 1300 nm with $R = 2.30\,\mu$m), and $N_r = 6$ ($D = 0 \pm 8.2$ ps/nm/km, wavelength bandwidth of 1340 nm with $R = 2.30\,\mu$m). This type of dispersion properties (oscillating near zero ultraflat dispersion PCF) is becoming an excellent candidate for broadband smooth supercontinuum generation (SCG) [22, 23] where flatness of the spectrum strongly depends on the dispersion nature [24]. Another interesting fact that can be observed from the dispersion figures is the presence of an almost "R independent dispersion". For $N_r = 3$, the corresponding wavelength comes around 1.32 μm (at least with the R values from 1.70 μm to 2.5 μm) with the crossing region of approximately 0.1 μm. There are similar regions for other cases with $N_r = 4$, $N_r = 5$, and $N_r = 6$ with the approximate value of the center wavelength of 1.306 μm, 1.305 μm, and 1.311 μm, respectively. So with the increment of N_r the "R independent dispersion" wavelength moves towards smaller wavelengths and then shifts to higher wavelength. However, the particular wavelength remains little perturbed with the change of N_r.

3.2. Loss of the Structure and Its N_r Dependence. For the above discussed almost flattened dispersion cases, the corresponding losses around C-band of wavelength are found out to be approximately 1.95×10^3 dB/m, 5.13×10^2 dB/m, 1.55×10^2 dB/m and 4.82×10^1 dB/m, for $N_r = 3$, $N_r =$

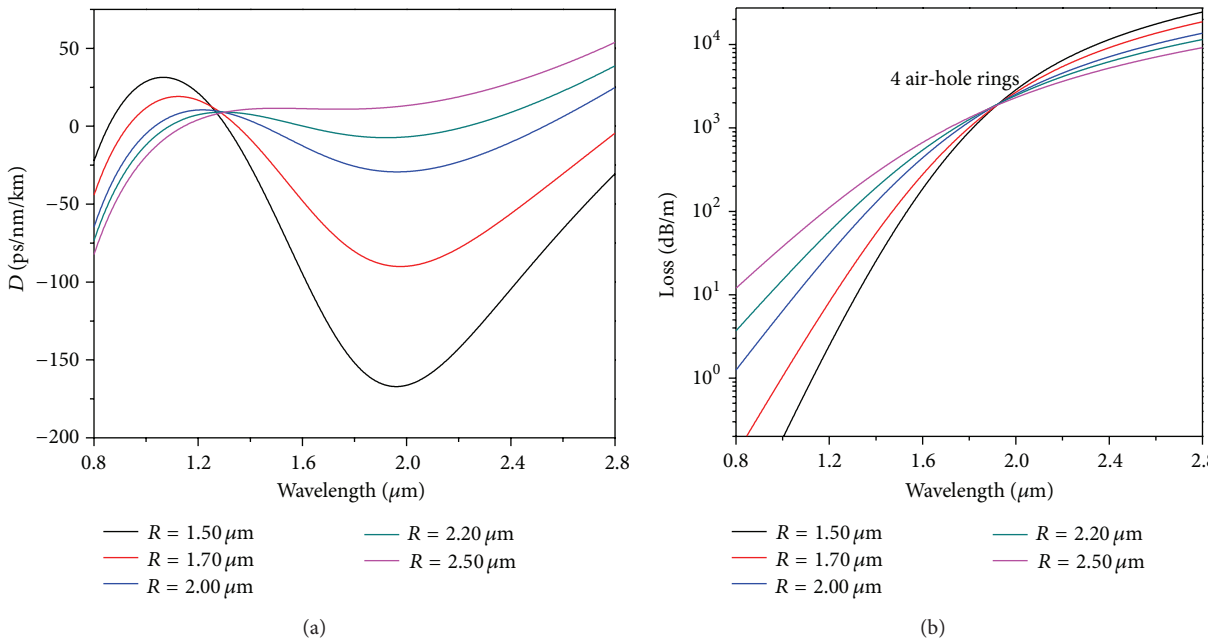

Figure 3: (a) Dispersion and (b) losses for different spacings of the circle (R) for four-ring C-PCF with air hole diameter $d = 0.8\,\mu$m.

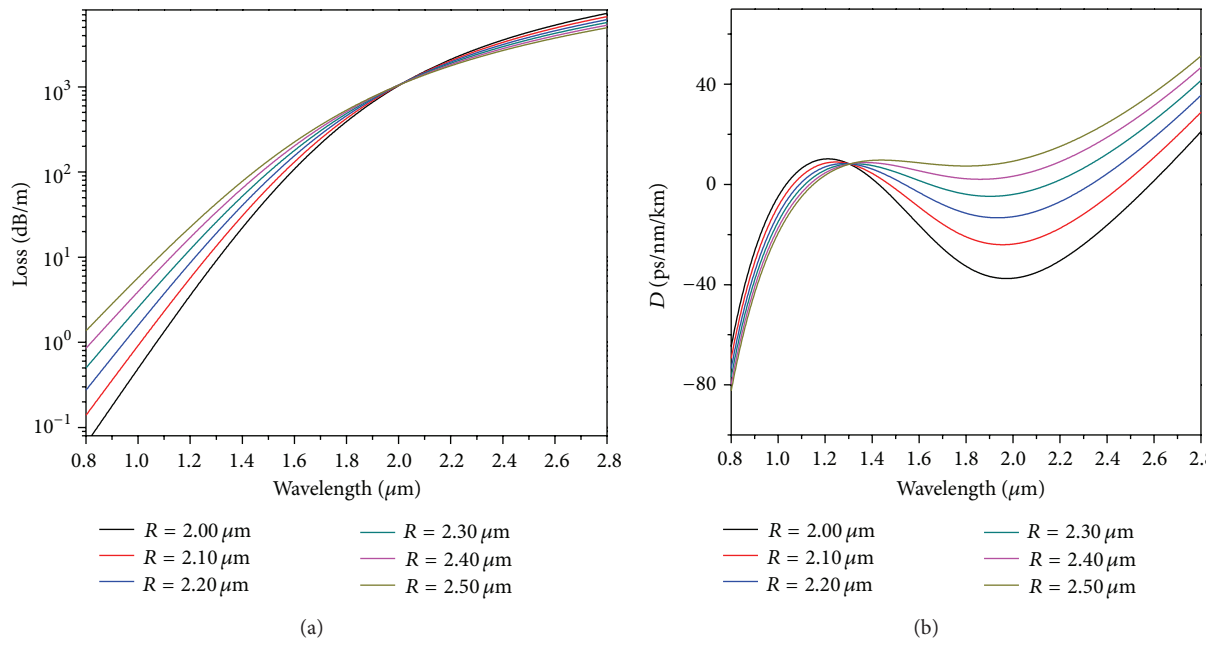

Figure 4: (a) Dispersion and (b) losses for different spacings of the circle (R) for five-ring C-PCF with air hole diameter $d = 0.8\,\mu$m.

4, $N_r = 5$, and $N_r = 6$ as shown in Figures 2(b), 3(b), 4(b), and 5(b), respectively. So, though we might be getting a flattened dispersion PCF, the design will not be suitable for practical applications as the losses are very high. However, for high power nonlinear applications like SCG and so forth, the pump wavelength is the wavelength of zero dispersion wavelength (ZDW) [24, 25]. For all the above cases, the values of ZDW come out to be 1.120 μm, 1.132 μm, and 1.134 μm and 1.136 μm, respectively. The corresponding losses around these wavelengths are 3.60×10^2 dB/m, 6.25×10^1 dB/m, 1.06×10^1 dB/m, and 1.81 dB/m, respectively. As high power nonlinear applications like SCG require even less than a meter long of the fiber [25], practical applications of the designed fiber are feasible especially with $N_r = 6$ and with $R = 2.6\,\mu$m as shown in Figure 5. The losses corresponding to first ZDW of the oscillating near-zero flat dispersion comes out to be 1.53×10^2 dB/m, 2.77×10^1 dB/m, 0.64×10^1 dB/m, and 0.94 dB/m for $N_r = 3$, $N_r = 4$, $N_r = 5$ and $N_r =$

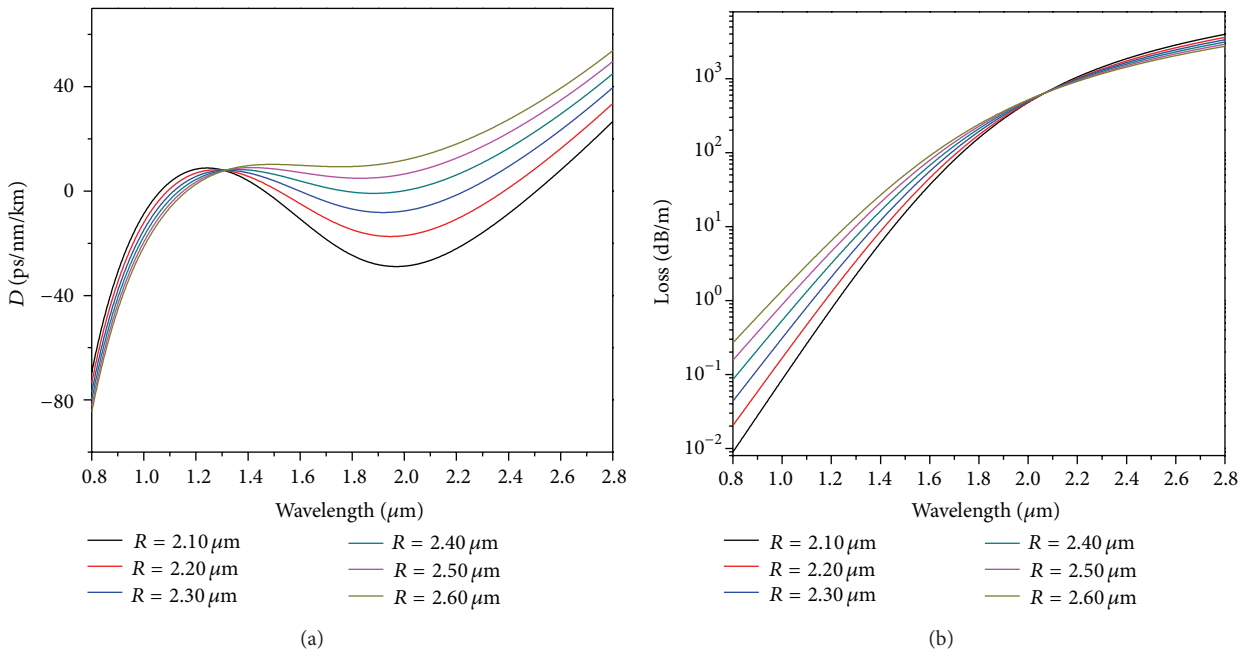

FIGURE 5: (a) Dispersion and (b) losses for different spacings of the circle (R) for six-ring C-PCF with air hole diameter $d = 0.8\,\mu$m.

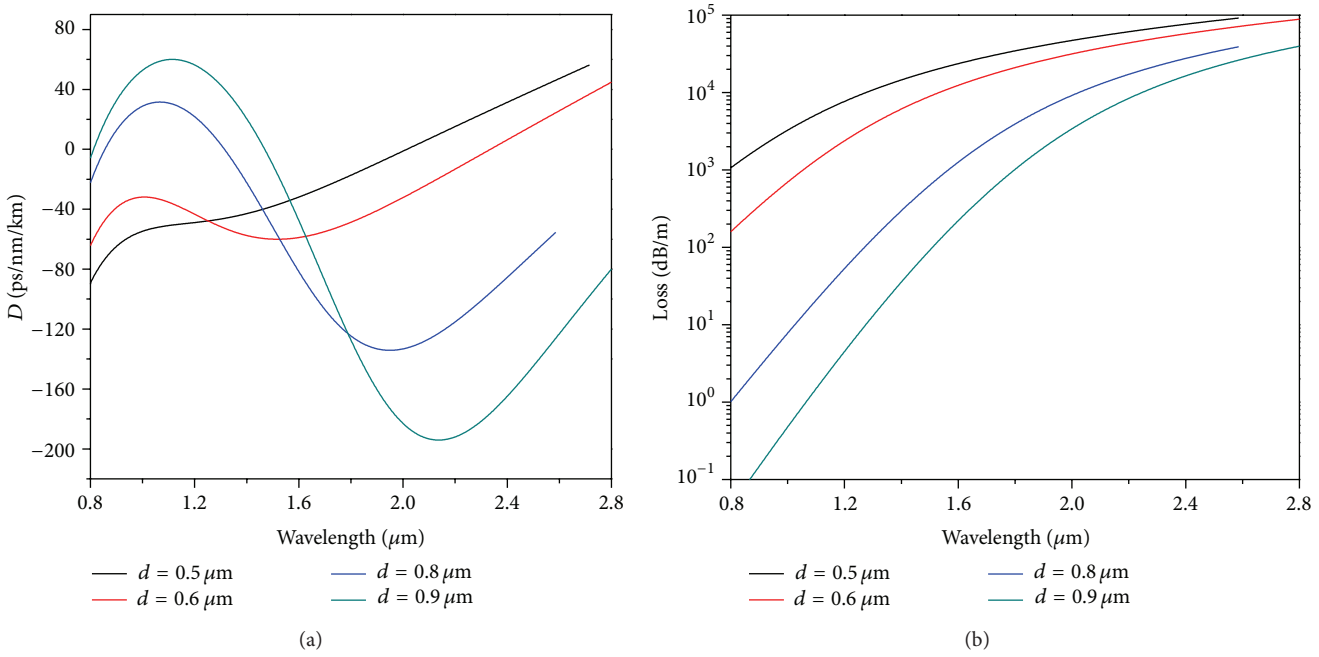

FIGURE 6: (a) Dispersion and (b) losses for a three-ring MOF for different air hole diameters d.

6 respectively. The above data shows that applications like broadband smooth SCG (where only a meter long of the fiber is required) are possible with $N_r = 6$ and with $R = 2.3\,\mu$m. The above results imply that the losses can be reduced by increasing N_r, but the dispersion nature will not remain the same. So to design a proper practical design we need to be careful for both the loss and dispersion. Similar to the case of R independent dispersion, another interesting fact that can be observed is the presence of "R independent loss" which is more prominent. The wavelength for "R independent loss" with 3 air hole rings comes out to be $1.79\,\mu$m, and the range for this wavelength is even less than $0.02\,\mu$m. Similar phenomenon can be observed for other values of air hole rings as well as with the wavelengths of $1.93\,\mu$m, $2.01\,\mu$m, and $2.07\,\mu$m for $N_r = 4$, $N_r = 5$ and $N_r = 6$ as can be observed from Figures 3(b), 4(b), and 5(b) respectively. Here

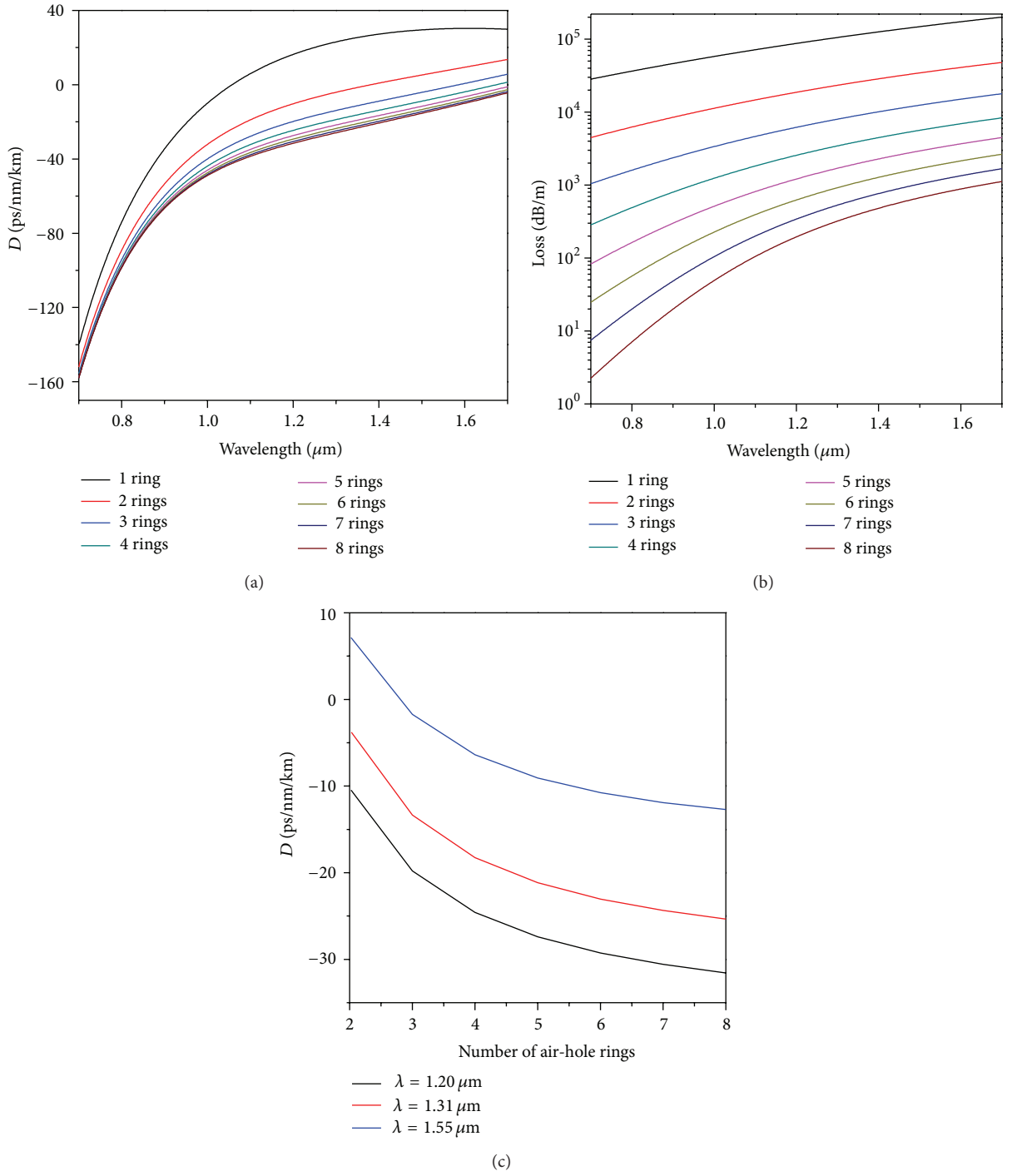

FIGURE 7: (a) Dispersion and (b) losses for different N_r for $R = 2.0\,\mu$m and $d = 0.5\,\mu$m. (c) Convergence for three different wavelengths for different numbers of air hole rings (N_r) for the above parameters.

the "R independent loss" wavelength gets red-shifted with the increase of N_r. Throughout the above designs we have considered the confinement losses of the structure; however, the sources of losses in MOFs can be limited by some other factors like structural imperfections, Rayleigh scattering, and absorption which are not affected by the geometrical losses.

3.3. Effect of Air Hole Diameter (d). In this section we will be discussing the effect of change of air hole diameter upon dispersion for a fixed value of circular spacing. Figure 5 shows the dispersion and loss characteristics for different values of air hole diameter keeping R (=1.50 μm), and N_r (=3) constant. Figure 6(a) dictates that the oscillation amplitudes

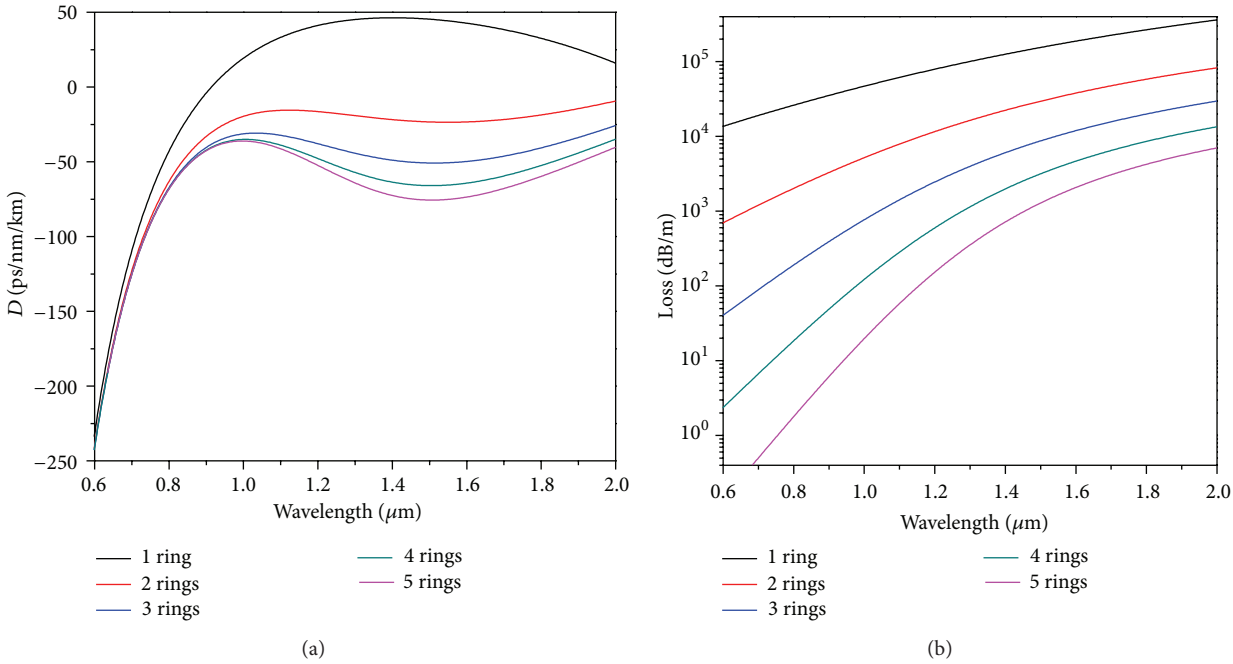

FIGURE 8: (a) Dispersion and (b) losses for different numbers of air hole rings. $R = 1.55\,\mu$m and $d = 0.60\,\mu$m.

in dispersion curves increase with air hole diameter. For $d = 0.90\,\mu$m, the oscillation amplitude becomes 250 ps/nm/km, whereas, for the smaller values of $d = 0.60\,\mu$m the amplitude of oscillation reduces to 30 ps/nm/km. These typical characteristics can be explained by considering the interplay between material dispersion and waveguide dispersion. For higher values of air hole diameter the waveguide dispersion dominates, whereas for smaller values of air hole diameter, material dispersion takes over the total dispersion. It is interesting to note that the value of $D_{\max}$ for a particular circular radius increases with the increase of air hole diameter. This is an important finding as the dispersion can be tailored according to the engineer's requirement for specific applications. The losses for the above-studied structures are presented in Figure 6(b). The loss gets reduced with the increase of air hole diameter as the mode becomes tightly confined.

3.4. Effect of Number of Air Hole Rings (N_r). In the following section, we discuss the effect of change of N_r. For this purpose we have subdivided the analysis into two sections. In the first case, we discuss the effect for smaller values of air-filling fraction such that material dispersion dominates the total dispersion and for this obvious reason we will not be having any local maxima in our dispersion curve. The effect has been shown in Figure 7. The dispersion decreases as N_r is increased as clearly shown in Figure 7(a). The difference between successive dispersion curves of two MOFs decreases as N_r increases, as shown in Figure 7(c). This figure clearly shows that the dispersion almost converges, when N_r is increased. This convergence depends upon the operating wavelength. The larger the wavelength, the higher the convergence, as shown in Figure 7(c). The graph clearly indicates that for $\lambda = 1.55\,\mu$m the limit is almost achieved, whereas for smaller wavelength ($\lambda = 1.20\,\mu$m) the convergence is yet to reach its limit even with $N_r = 8$. This factor is different to that of regular triangular PCF [3]. The losses with higher N_r, say for 8 rings, are still higher as shown in Figure 7(b).

We now switch to the second case, where we have considered higher air-filing fraction so that we are having oscillating nature in the dispersion characteristics. For this purpose, we have considered $R = 1.55\,\mu$m with $d = 0.6\,\mu$m. With the increase of N_r, the oscillation amplitude increases and the negative dispersion value also increases as shown in Figure 8(a). This is due to the increasing effect of waveguide dispersion in the total dispersion. The losses for the above cases are presented in Figure 8(b), which clearly shows that the performance respect losses improve with the increase of air hole rings. The above influence can be explained on the basis of the mode confinement. When the mode is well confined to the core, an additional air hole ring is not going to change the modal properties drastically, whereas for the reverse case for a loosely bound mode an additional air hole ring is going to affect its modal properties significantly and we can expect the field pattern associated with the mode to converges with the increase of air hole ring.

4. Conclusion and Discussion

We carried out a detail numerical analysis of the dispersion and loss characteristics of a new type of photonic crystal fiber where air holes are arranged in a circular pattern. Influence of different geometrical parameters, namely, the circular spacing, air hole diameter, and number of air hole rings has been carried out in detail. Total dispersion is strongly affected by the interplay between material dispersion

and waveguide dispersion. For smaller air-filing fraction, adding extra air hole rings does not change dispersion much whereas, for higher air-filling fraction, the dispersion nature changes significantly. With proper adjustment of the available parameters, ultraflat dispersion (dispersion fluctuation of 0.35 ps/nm/km around 1.65 μm) for a broad wavelength band could be achieved, though the practical applications around C-band are limited due to the higher loss. However, for high power applications like SCG and so forth where less than a meter of the fiber is sufficient, the ultraflat dispersion fiber will be suitable with the low loss at the first ZDW. We also achieved small oscillating ($D = 0 \pm 8.2$ ps/nm/km) near-zero dispersion, and the design will be helpful for broadband smooth SCG (where only a meter long of the fiber is required) as the loss at the first ZDW comes out to be 0.95 dB/m. It has been shown that, for increased number of air holes, the dispersion tends to saturate. The saturation is sensitive for different wavelengths, and the saturation improves at higher wavelengths. The detailed study shows that for realistic dispersion engineering, we need to be careful for both the loss and dispersion.

Conflict of Interests

The authors would like to declare that there is no direct financial relation with any commercial identity mentioned in their work that might lead to a conflict of interests.

Acknowledgments

The authors would like to thank Dr. Boris Kuhlmey, University of Sydney, Australia, for providing valuable suggestions in understanding the software for designing and studying the properties of different structures. The authors acknowledge sincerely the Defence Research and Development Organization, Government of India, and CRF of IIT Kharagpur for the financial support to carry out this research.

References

[1] J. C. Knight, "Photonic crystal fibers," *Nature*, vol. 424, pp. 847–851, 2003.

[2] P. S. J. Russell, "Photonic-crystal fibers," *Journal of Lightwave Technology*, vol. 24, no. 12, pp. 4729–4749, 2006.

[3] B. T. Kuhlmey, G. Renversez, and D. Maystre, "Chromatic dispersion and losses of microstructured optical fibers," *Applied Optics*, vol. 42, no. 4, pp. 634–639, 2003.

[4] A. H. Bouk, A. Cucinotta, F. Poli, and S. Selleri, "Dispersion properties of square-lattice photonic crystal fibers," *Optics Express*, vol. 12, no. 5, pp. 941–946, 2004.

[5] W. H. Reeves, J. C. Knight, P. S. J. Russell, and P. J. Roberts, "Demonstration of ultra-flattened dispersion in photonic crystal fibers," *Optics Express*, vol. 10, no. 14, pp. 609–613, 2002.

[6] K. Saitoh, M. Koshiba, T. Hasegawa, and E. Sasaoka, "Chromatic dispersion control in photonic crystal fibers: application to ultra-flattened dispersion," *Optics Express*, vol. 11, no. 8, pp. 843–852, 2003.

[7] P. S. Maji and P. R. Chaudhuri, "A new design of ultra-flattened near-zero dispersion PCF using selectively liquid infiltration," *Journal of Photonics and Optoelectronics*, vol. 2, pp. 25–32, 2013.

[8] X. Zhao, G. Zhou, L. Shuguang et al., "Photonic crystal fiber for dispersion compensation," *Applied Optics*, vol. 47, no. 28, pp. 5190–5196, 2008.

[9] S. Yang, Y. Zhang, X. Peng et al., "Theoretical study and experimental fabrication of high negative dispersion photonic crystal fiber with large area mode field," *Optics Express*, vol. 14, no. 7, pp. 3015–3023, 2006.

[10] F. Gérôme, J. L. Auguste, and J. M. Blondy, "Design of dispersion-compensating fibers based on a dual-concentric-core photonic crystal fiber," *Optics Letters*, vol. 29, no. 23, pp. 2725–2727, 2004.

[11] W. D. Ho, T. W. Lu, Y. H. Hsiao, and P. T. Lee, "Thermal properties of 12-fold quasi-photonic crystal microcavity laser with size-controlled nano-post for electrical driving," *Journal of Lightwave Technology*, vol. 27, no. 23, pp. 5302–5307, 2009.

[12] N. Horiuchi, Y. Segawa, T. Nozokido, K. Mizuno, and H. Miyazaki, "High-transmission waveguide with a small radius of curvature at a bend fabricated by use of a circular photonic crystal," *Optics Letters*, vol. 30, no. 9, pp. 973–975, 2005.

[13] P. T. Lee, T. W. Lu, J. H. Fan, and F. M. Tsai, "High quality factor microcavity lasers realized by circular photonic crystal with isotropic photonic band gap effect," *Applied Physics Letters*, vol. 90, no. 15, Article ID 151125, 2007.

[14] W. Zhong and X. Zhang, "Localized modes in defect-free two-dimensional circular photonic crystals," *Physical Review A*, vol. 81, no. 1, Article ID 013805, 6 pages, 2010.

[15] H. Xu, J. Wu, K. Xu, Y. Dai, C. Xu, and J. Lin, "Ultra-flattened chromatic dispersion control for circular photonic crystal fibers," *Journal of Optics*, vol. 13, no. 5, Article ID 055405, 2011.

[16] A. Argyros, I. M. Bassett, M. A. van Eijkelenborg et al., "Ring structures in microstructured polymer optical fibres," *Optics Express*, vol. 9, no. 13, pp. 813–820, 2001.

[17] CUDOS MOF Utilities, http://sydney.edu.au/science/physics/cudos/research/mofsoftware.shtml.

[18] T. P. White, B. T. Kuhlmey, R. C. McPhedran et al., "Multipole method for microstructured optical fibers. I. Formulation," *Journal of the Optical Society of America B*, vol. 19, no. 10, pp. 2322–2330, 2002.

[19] B. T. Kuhlmey, T. P. White, G. Renversez et al., "Multipole method for microstructured optical fibers. II. Implementation and results," *Journal of the Optical Society of America B*, vol. 19, no. 10, pp. 2331–2340, 2002.

[20] T. A. Birks, J. C. Knight, and P. S. J. Russell, "Endlessly single-mode photonic crystal fiber," *Optics Letters*, vol. 22, no. 13, pp. 961–963, 1997.

[21] J. M. Dudley and J. R. Taylor, "Ten years of nonlinear optics in photonic crystal fibre," *Nature Photonics*, vol. 3, no. 2, pp. 85–90, 2009.

[22] K. Saitoh and M. Koshiba, "Highly nonlinear dispersion-flattened photonic crystal fibers for supercontinuum generation in a telecommunication window," *Optics Express*, vol. 12, no. 10, pp. 2027–2032, 2004.

[23] F. Begum, Y. Namihira, T. Kinjo, and S. Kaijage, "Supercontinuum generation in square photonic crystal fiber with nearly zero ultra-flattened chromatic dispersion and fabrication tolerance analysis," *Optics Communications*, vol. 284, no. 4, pp. 965–970, 2011.

[24] J. M. Dudley, G. Genty, and S. Coen, "Supercontinuum generation in photonic crystal fiber," *Reviews of Modern Physics*, vol. 78, no. 4, pp. 1135–1184, 2006.

[25] S. Roy and P. R. Chaudhuri, "Supercontinuum generation in visible to mid-infrared region in square-lattice photonic crystal fiber made from highly nonlinear glasses," *Optics Communications*, vol. 282, no. 17, pp. 3448–3455, 2009.